The VEI-7 Millennium eruption, Changbaishan-Tianchi volcano, China/DPRK: New field, petrological, and chemical constraints on stratigraphy, volcanology, and magma dynamics

Article *in* Journal of Volcanology and Geothermal Research · June 2017
DOI: 10.1016/j.jvolgeores.2017.05.029

CITATION
1

READS
154

6 authors, including:

Bo Pan
Institute of Geology, China Earthquake Administration
2 PUBLICATIONS **1** CITATION
SEE PROFILE

Shanaka de Silva
Oregon State University
134 PUBLICATIONS **2,820** CITATIONS
SEE PROFILE

Xu Jiandong
China Earthquake Administration
64 PUBLICATIONS **452** CITATIONS
SEE PROFILE

Zhengquan Chen
Institute of Geology, China Earthquake Administration
10 PUBLICATIONS **18** CITATIONS
SEE PROFILE

Journal of Volcanology and Geothermal Research 343 (2017) 45–59

Contents lists available at ScienceDirect

Journal of Volcanology and Geothermal Research

journal homepage: www.elsevier.com/locate/jvolgeores

The VEI-7 Millennium eruption, Changbaishan-Tianchi volcano, China/DPRK: New field, petrological, and chemical constraints on stratigraphy, volcanology, and magma dynamics

Bo Pan [a,b,*], Shanaka L. de Silva [b], Jiandong Xu [a], Zhengquan Chen [a], Daniel P. Miggins [b], Haiquan Wei [a]

[a] Key Laboratory of Active Tectonics and Volcano, Institute of Geology, China Earthquake Administration, Beijing 100029, China
[b] College of Earth, Ocean, and Atmospheric Sciences, Oregon State University, Corvllis, OR 97333, United States

ARTICLE INFO

Article history:
Received 13 February 2017
Received in revised form 23 May 2017
Accepted 24 May 2017
Available online 7 June 2017

Keywords:
Changbaishan-Tianchi
Millennium eruption
Revised stratigraphy
Magma mixing
Magma dynamics

ABSTRACT

Field relations, petrography, bulk and micro-scale chemistry reveal that the most recent history of hazardous Changbaishan-Tianchi volcano should be revised with important implications for volcanic hazard in NE Asia. Currently, the two most recent large eruptions are identified separately as a VEI 5 trachytic Baguamiao eruption (BGM) and the much heralded VEI 7, late 946 CE (Common Era) "Millennium" eruption (ME) of comendite. However, we find that the former is part of the latter based on the following evidence: (1) trachytic fallout of the BGM lies directly on the comendite tephra of the ME without any indication of depositional hiatus; (2) abundant mingled trachyte-comendite pumice in the tephra deposits; (3) similar chemistry of mingled pumice and its components to those in the BGM and ME products; (4) correlation of bimodal glass shard compositions in the distal 'B-Tm' ash from the Japan Sea with comendite and trachyte glass from the BGM and ME products. Based on the above evidence, we suggest that the great Millennium eruption of 946 CE should be revised finally to include the BGM trachyte as its final stage. Furthermore, deposits attributed to two other trachytic eruptions in 1668 and/or 1702 CE (also called Baguamiao by some authors), and 1903 CE referred to in historic accounts were also examined. Our field observations, petrography, bulk and micro-scale chemistry combined with previously published Ra/Th ages indicate that all these trachytes are either primary deposits of the ME or its reworked deposits. Thus our findings do not support two separate post-ME eruptions and require that volcanic hazard assessment at Changbaishan volcano include this new interpretation.

Recently published geochronological data integrated with our new petrochemical and volcanological framework informs the magma dynamics leading to the ME. The ME comendite, derived from a parental trachyte similar to the BGM started accumulating at shallow levels around 12 ka to 8 ka. Around 4 to 1.6 ka the BGM trachyte sensu *strictu* separated from its basaltic parent and started accumulating and crystallizing separately from the ME comendite. Just prior to the ME eruption, mingling of trace amounts of a third more mafic hybrid is implicated by the composition of mafic glass selvedges. The strong evidence for mixing of all these endmembers in the eruption products suggests that recharge mixing and overturn of this predominantly comendite-trachyte system occurred during the ~1 ka ME. The common occurrence of comendite and trachyte in the last 100 ka (also maybe 1 Ma) at Changbaishan-Tianchi suggests that conditions for trachyte-comendite magma interactions are prevalent in the magma system of Changbaishan and maybe crucial in catastrophic eruptions there.

1. Introduction

The 946 CE (Common Era) Millennium eruption (ME) from Changbaishan-Tianchi volcano, China/Democratic People's Republic of Korea (DPRK) (Machida and Arai, 1983; Oppenheimer, 2011; Xu et al., 2013; Oppenheimer et al., 2017) is heralded as Asia's largest historical eruption, that, with a magnitude of 7.4 (Magnitude M of Pyle, 2000), is one of the two largest explosive eruptions in the Holocene on Earth (Crosweller et al., 2012; Brown et al., 2015). Ash fallout from the eruption has been traced to northern Japan and the Kurile trench (Fig. 1: Machida and Arai, 1983; Horn and Schmincke, 2000; Nanayama et al., 2003). An earlier major explosive eruption, the Tianwenfeng eruption has ages ranging from ~40 to 70 ka, produced the Yellow pumice which can be traced eastwards into the Japan Sea as Baitoushan-Japan ash (B-J), is also known (Chun et al., 2006). This history of major explosive eruptions and recent swarms of seismic tremor between 2002 and 2006 has established Changbaishan-Tianchi as the most dangerous

* Corresponding author at: Institute of Geology, China Earthquake Administration, Huayanli A01, Chaoyang District, 100029 Beijing, China.
E-mail addresses: dujushi1981@163.com, panbo@ies.ac.cn (B. Pan).

http://dx.doi.org/10.1016/j.jvolgeores.2017.05.029
0377-0273/

volcano in China (Xu et al., 2012) and efforts to understand the hazard are redoubling (Stone, 2011, 2013).

An unresolved debate that complicates hazard assessment at Changbaishan is about the most recent eruptive history. Several post-ME eruptions are based on remote historical accounts and proxy records (Siebert et al., 2010; Yun, 2013; Ramos et al., 2016; Table 1). Many of these are of dubious veracity, yet have been taken at face value and used to establish the eruption history (Supplementary S1 and Table 1). Most previous studies focused on single sample age determinations of the ME and are based on limited field constraints to inform the stratigraphy (Table 1). At the center of the debate are the trachytic deposits that overlie the comenditic products of the ME. Largely based on the records of the Korean Kingdom that describe a "rain with ash" on Xianjing province (~200 km distant from Tianchi caldera), the trachytic tephra was ascribed to the Baguamiao eruption (BGM) and an age of 1668 and/or 1702 CE (Jin and Cui, 1999; Liu et al., 1998; Yun, 2013). Estimated as a ~VEI 5, this suggested a significant explosive eruption about 350 years ago. Additionally, reports of a "gas ejection from the volcano" in 1903 CE has been taken as evidence of an eruption at that time and trachytic "maar" deposits at the lake shore were attributed to this event (Wei et al., 2013). Recent Ra/Th model ages have been shown to agree with these proxy dates (Ramos et al., 2016) although it is acknowledged that these are all controversial.

There is other research that has interpreted all the uppermost trachytic deposits around the caldera as the late stage of the Millennium eruption (Dunlap, 1996; Tokui, 1989; Horn and Schmincke, 2000). However, these efforts have been largely ignored in more recent work and several outcrops of the most recent deposits at Tianchi have been ascribed to a 1668 and/or 1702 CE Baguamiao eruption, as well as to a separate 1903 CE eruption. The possible existence of these post-ME eruptions now imposes a significant influence on hazard assessment at Changbaishan (e.g. Wei et al., 2013).

In an effort to resolve this debate, we have investigated the relationship between all these deposits and present here new field, petrological, and geochemical evidence for an explicit link between them that confirms they are all part of the ME. We then use this new volcanological framework (Table 1) to inform the magma dynamics that leads to catastrophic eruptions at Changbaishan volcano.

2. Geologic background

Changbaishan is a volcanic complex built upon the 29 Ma Gaima basalt plateau on the northern edge of the Archean-Proterozoic Sino-Korean craton (Liu et al., 1998; Wei et al., 2013). Three large composite volcanoes compose Changbaishan. The oldest is Baotaishan volcano in DPRK, then the Wangtiane volcano in China (5–2 Ma), finally followed by the Tianchi volcano (2 Ma-present) straddling the border (Fan et al., 2007). Tianchi (Heavenly Lake) volcano itself has undergone three evolutionary stages: the lower basaltic shield formation (2 Ma–1 Ma), a middle comenditic and trachytic composite cone formation (1 Ma–0.04 Ma), and the latest explosive ignimbrite-stage during which comendite (rhyolite) and trachyte magma was erupted (Fan et al., 2007; Wei et al., 2007, 2013; Fig. 2). The overall trend from early alkali basalt to trachyte-comendite has been attributed to crystal-

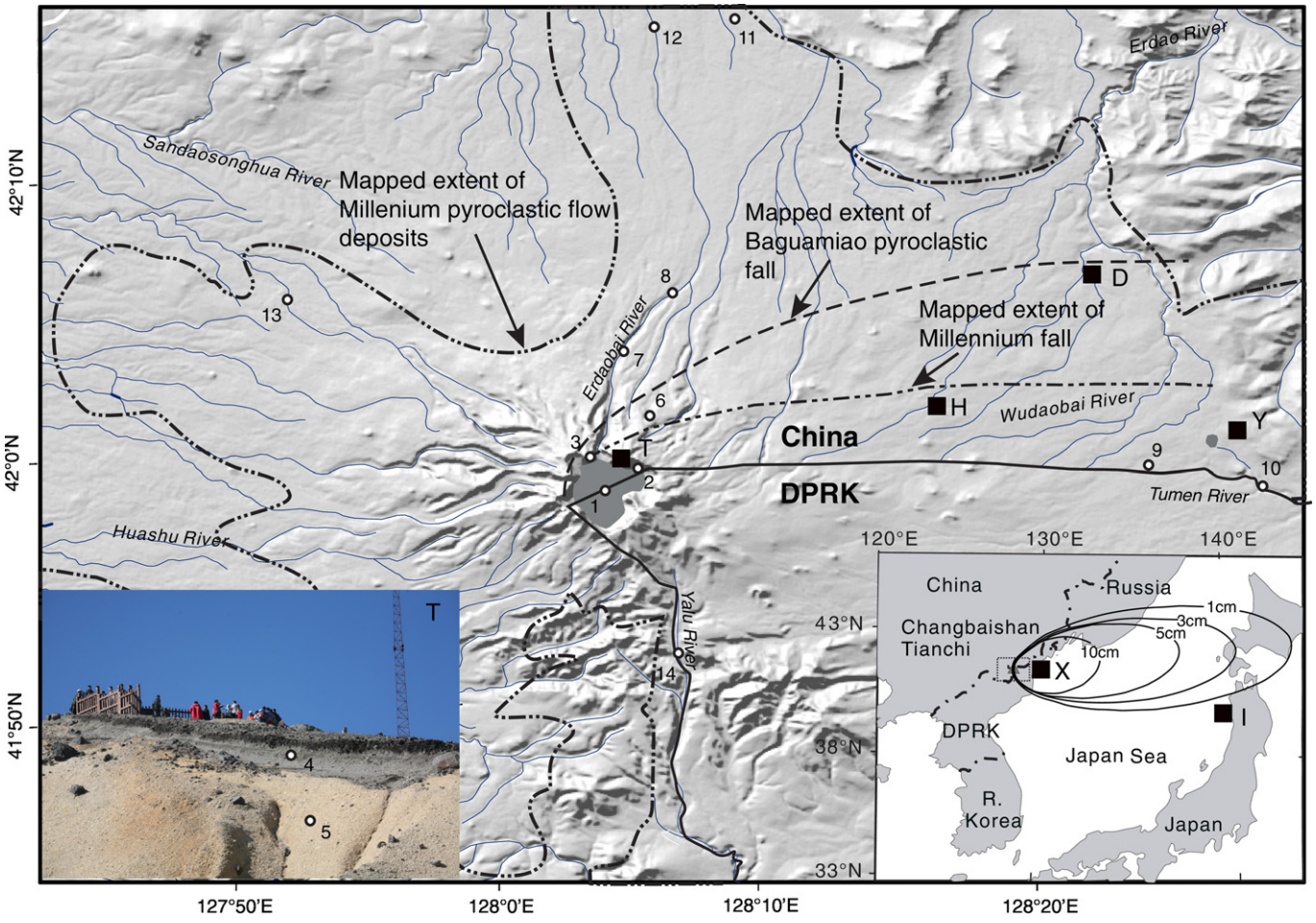

Fig. 1. Location map of Tianchi volcano, Changabaishan volcanic complex showing the mapped distribution of the "Millennium" pyroclastic flow deposits and the Baguamiao fallout deposit are shown. Note that the no information is available from DPRK. Field sites are indicated and those referred to in the text are same as in the caption of Table 1. Area of the main map is shown in the inset map.

Table 1
Summary of the chronostratigraphy of the most recent history of Changbaishan Tianchi volcano eruption.

Author	This paper			Ramos et al. (2016)			Liu, et al. (2004)			Liu (2000)			Jin, et al. (2000)			Cui (1997)			Jin and Zhang (1994)			Xu, et al. (1993)		
	Name	Des/Loc	Age	Name	Des/Loc	Age	Name	Des /Loc	Age	Name	Des /Loc	Age	Name	Des /Loc	Age	Name	Des /Loc	Age	Name	Des /Loc	Age	Name	Des /Loc	Age
1	ME Second stage (Trachyte)	Black tuff and ignimbrite /2/3/8/14	946±3 AD	Liuhaojie	Grey and Black pumice /2	1903 AD (?)	Yuanchi	Black tuff /3	1199-1200 AD	History record	Black ignimbrite /3	1668, 1702 AD	History record	Gas /1	0.3ka BP	Tianchi	Gas /1	0.09-0.3 ka BP	History record	Gas /1	1903, 1702, 1668, 1597AD	Liuhaojie	Black tuff /2	<1ka
2		Dark pumice /2/4/9		BGM	Black pumice /3	1668 AD (?)		Grey pumice /4		ME	Grey pumice /4/9/10	1215±15 AD	BGM	Black ignimbrite /3	0.4-1ka BP	Naitoushan	Grey pumice /11	1ka BP	BGM	Black tuff /3	1167, 1117AD	Naigou	Black tuff /14	
3	ME First stage (Comendite)	Grey ignimbrite /9/11/12/D		ME	Grey and black pumice /4	946 AD		Yellow pumice /5		QXZ	Lava flow /6	4ka BP	BYF	Grey pumice /4	1-2ka BP	Xiaoshahe	Pyroclastic flow /13	1.4ka BP	BYF	Grey pumice /4	1489±70 a BP	QXZ	Lava flow /6	
4		Grey pumice fall /4/10/Y		QXZ	Spatter lava flow /6	No	Chifeng	Erdaobaihe Lahar /12		TWF	Yellow pumice /5	5ka BP	BC	Black tuff /7	3.5-7.8 ka BP	Erdaobaihe	Scoria, pumice /8	3.45ka BP		Yellow pumice /5		BGM	Black tuff /3	
5	QXZ	Spatter lava flow /6	~11ka BP	TWF	Yellow pumice /5	>4ka BP		Grey ignimbrite /9						Yellow pumice /5		Yuanchi	Grey pumice /9	6,44ka BP		Dark scoria /T	3450±200a BP	BYF	Grey pumice /4	1ka BP
6	TWF	Yellow pumice /5	~50ka BP					Pumice fall /10					QXZ	Lava flow /6	97.8-1ka BP	BC	Black ignimbrite /7	7.8ka BP		Grey pumice /T	6440±110a BP		Yellow pumice /5	
7							QXZ	Lava flow /6	4-18 ka BP								Yellow pumice /5		BC	Black tuff /7	7822±210a BP			

Des, Description for deposit; Loc, Location or position. Light grey, deposit of the ME first stage (comendite) in this paper; dark Grey, deposit of the ME second stage (trachyte) in this paper. Number and Letters refer to locations, units, and events on Fig. 1: 1, Tianchi (Gas release); 2, Liuhaojie(1903 CE); 3, Baguamiao (1668/1702 CE); 4, Grey pumice at Tianwenfeng summit; 5, Yellow pumice at Tianwenfeng summit; 6, Qixiangzhan lava flow; 7, Bingchang; 8, Erdaobaihe; 9, Yuanchi; 10, Chifeng; 11, Naitoushan; 12, Erdaobaihe lahar; 13, Xiaoshahe; 14, Naigou; T, Tianwenfeng summit; H, Heishigou trench; Y, Yuanchi trench; D, Dongfanghong; I, Japan Sea; X, Xianjing Province in DPRK. Abbreviation: BGM, Baguamiao eruption; ME, Millennium eruption; QXZ, Qixiangzhan eruption; TWF, Tianwefeng eruption; BC, Bingchang eruption; BYF, Baiyunfeng.

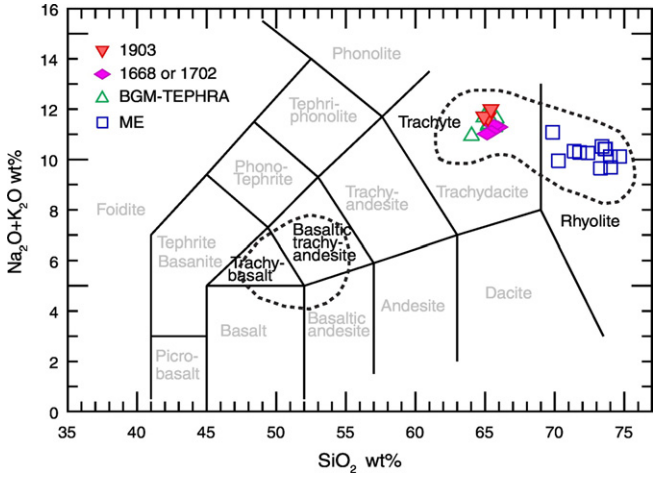

Fig. 2. Total alkali versus silica (TAS) classification diagram for volcanic rocks from Changbaishan-Tianchi volcano. Dashed shapes outline fields defined by previously published data for bulk rock compositions at Tianchi volcano (Fan, 2008; Liu et al., 1998). The symbols plotted are data obtained for this paper and reported in Supplementary File S2. BGM–Baguamiao; ME–Millennium.

fractionation, magma recharge and mixing (Dunlap, 1996; Liu et al., 1998; Fan, 2008).

A close association of trachyte and comendite magma during the last 100 ka at least of the Tianchi volcano is clear. For instance, the aforementioned middle stage of composite cone formation extending back to ~1 Ma, has multiple alternations of comendite to trachyte throughout the stratigraphy (Liu et al., 1998). Furthermore, mingling of comendite and trachyte can be found in the products of explosive eruptions at Changbaishan, but few of these eruptions have been studied to date. The best documented occurrence is in the extensive comendite fallout and regionally extensive ignimbrite of the ME and the overlying trachytic BGM fallout deposit (Dunlap, 1996; Liu et al., 1998; Horn and Schmincke, 2000).

The 5.5 km diameter Tianchi caldera is thought to have formed during the ME. A sustained plinian eruption column is estimated to have reached heights of at least 25 km (Horn and Schmincke, 2000; Yu et al., 2012). The resulting fallout deposit is found to the east in China and DPRK and has been correlated as far as northern Japan and the Kurile trench (~2000 km) where a 2–10 cm thick deposit of ash is recorded (Machida and Arai, 1983; Machida, 1999; Horn and Schmincke, 2000; Okuno et al., 2011; Nanayama et al., 2003) (Fig. 1). An energetic pyroclastic flow covered most of the area to the north and northeast area of Tianchi and filled the canyons around the caldera as far as 50 km (Fig. 1). The ME deposits are well exposed in China and in DPRK (Horn and Schmincke, 2000). The deposit attributed to the BGM is a fallout deposit of black or dark trachytic pumice, distributed on the crater rim and to the northeast of Tianchi (Fig. 1). Details of the ME and BGM deposits in the DPRK are unavailable at the time of writing.

3. Methods

The stratigraphy of the ME and BGM deposits was examined in sections and trenches at over forty locations in Chinese territory throughout the area to the northeast of Tianchi volcano (Fig. 1). Where possible, at each profile, pumice from both the ME and BGM were collected separately. Each of the known deposits attributed to the 1668/1702, and 1903 CE events were also examined and primary juvenile clasts collected. For the purposes of this project, ten ME, nine BGM, from widely spaced locations throughout the region were chosen for

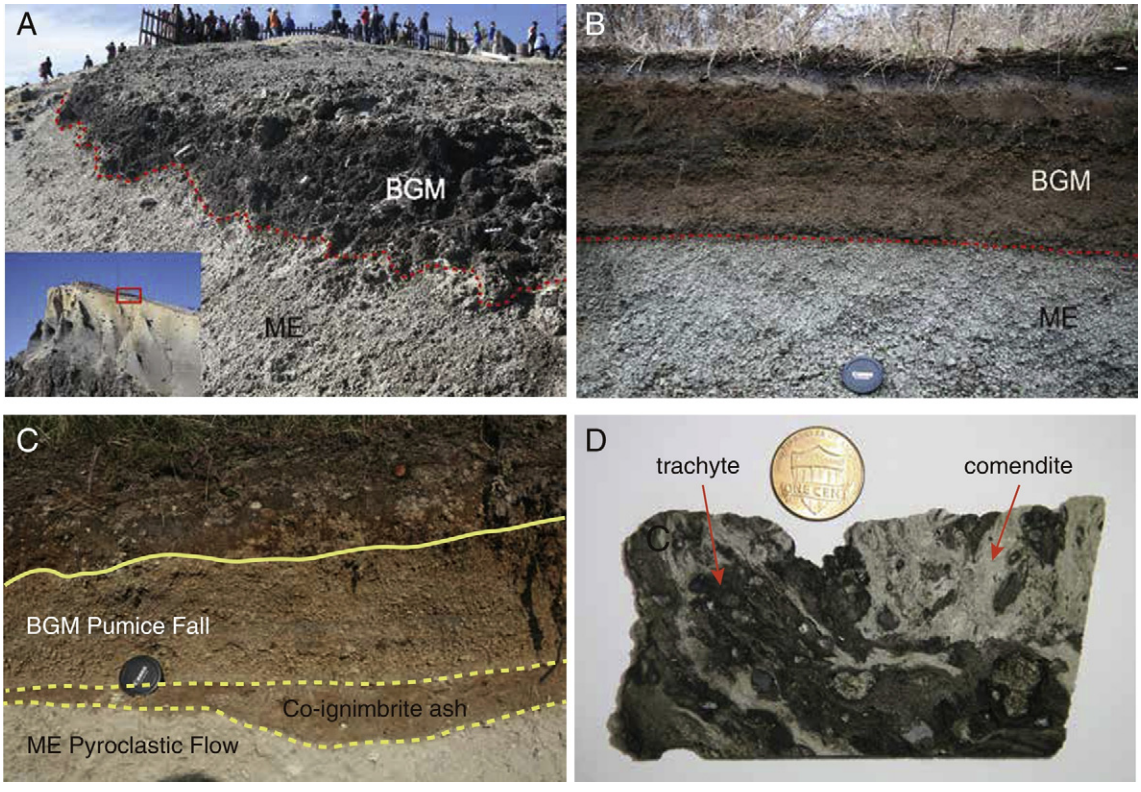

Fig. 3. Outcrop scale contact relations of Millennium (ME) and Baguamiao (BGM) deposits. A. Proximal section of Tianchi stratigraphy at Tianwenfeng on the northern crater rim (point T in Fig. 1), showing the contact between the dark trachyte of the BGM and the light-grey of the ME tephra. No depositional break is found but there is a clear compositional difference. B. Exposure at Yuanchi (point Y in Fig. 1) showing the BGM tephra directly on the grey ME tephra without any intervening deposits. C. Contact at Dongfang (point D in Fig. 1) showing the BGM pumice fallout deposit on the ME pyroclastic flows. Here a fine-ash fall-out (co-ignimbrite) of the ME comendite separates the two deposits. D. Mingled trachyte-comendite clast as seen in the upper part of the ME and throughout the BGM deposits. This particular example is from Heishi (point H in Fig. 1) and exhibits wisps and streaks of black trachyte and grey comendite mixed at different scales.

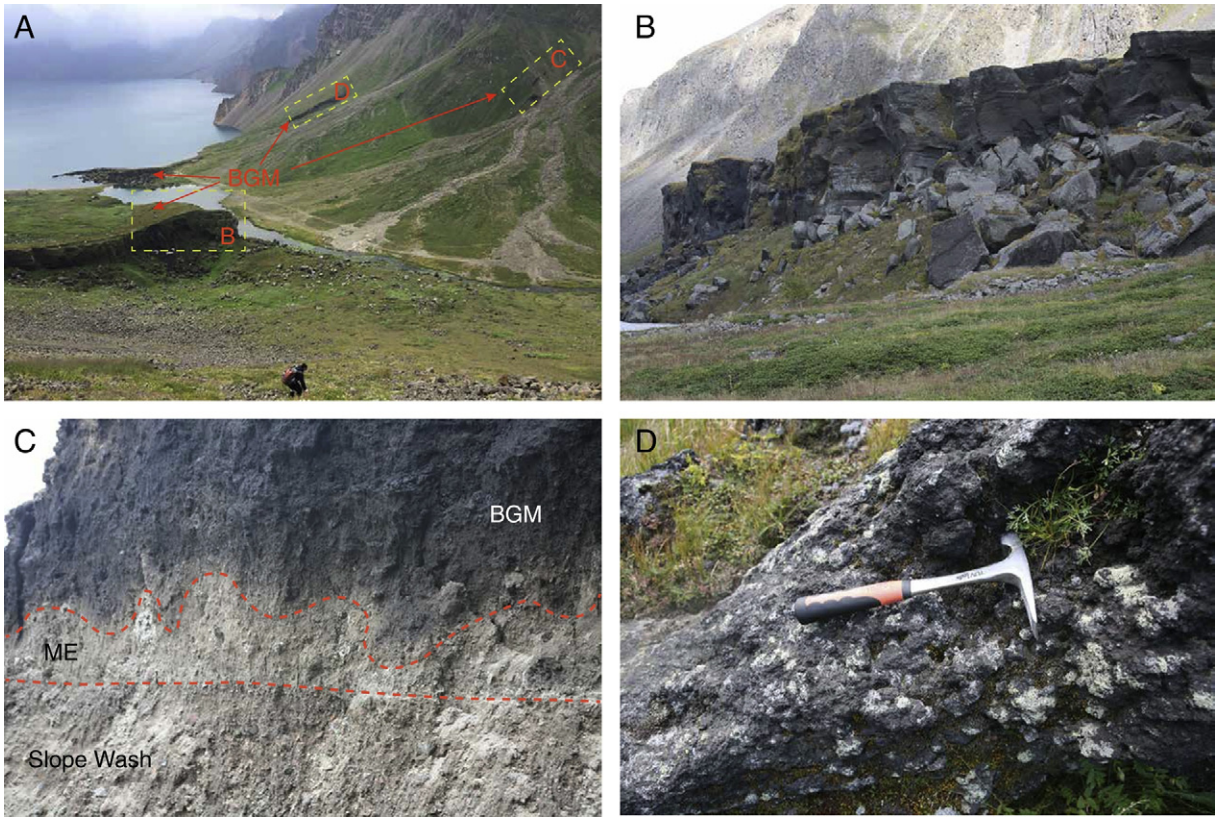

Fig. 4. Field photographs of supposed 1668/1702 CE deposits (point 3 in Fig. 1). A. The perspective view of 1668/1702 CE deposits in the northwest of the inner caldera. Lake Tianchi in the background. B. The black welded pyroclastics deposits of supposed 1668/1702 CE deposit about 20 m thick on the east bank of Chengcha river. C. Contact (point C in Fig. 4A) showing the 1668/1702 CE BGM black scoria lie on the ME deposit with gradual transformation. D. Close up (point D in Fig. 4A) for black and welded of 1668/1702 CE BGM scoria.

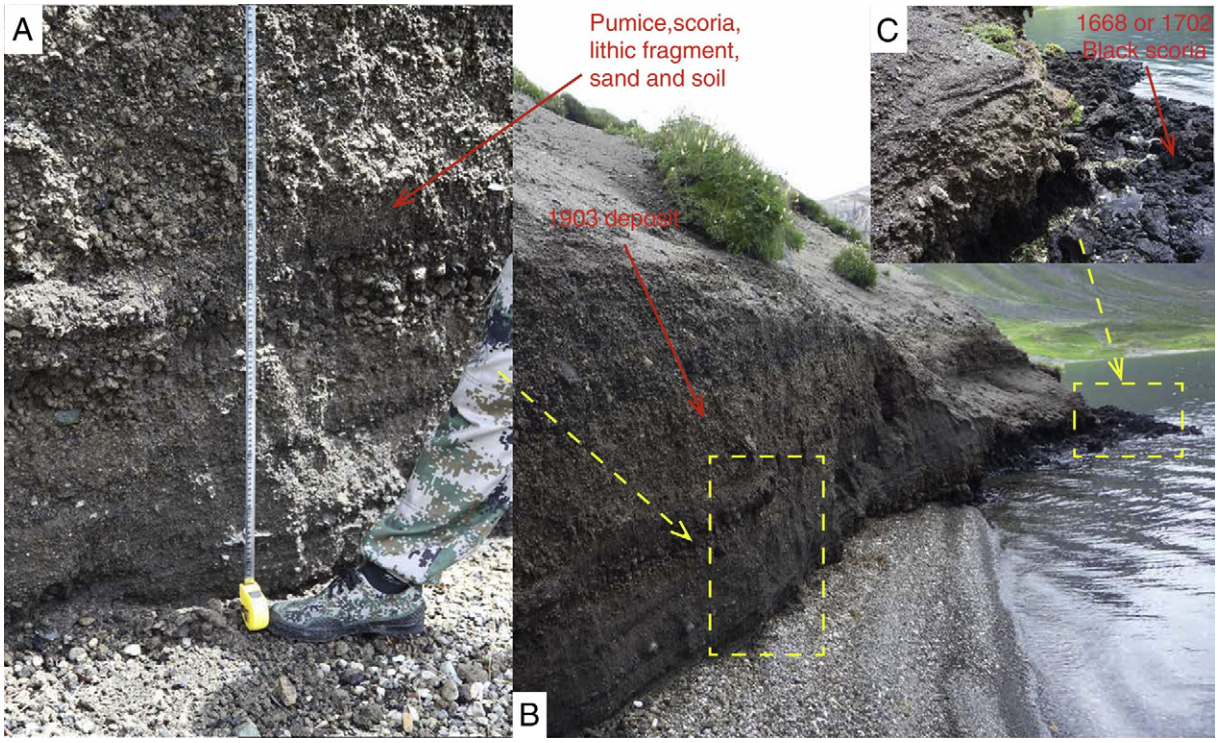

Fig. 5. Field photographs of supposed 1903 CE deposits (point 2 in Fig. 1). A. Close up of 1903 CE deposit showing the heterolithic sandy matrix-supported coarsely bedded to massive deposits. These consist of pumice, scoria, lithic fragments, in a matrix of sand and mud. No primary proximal welded deposits are found. B. The photograph showing 1903 CE reworked deposits lying on the 1668/1702 CE black welded deposits (see Fig. 4) on the northeast shore of Tianchi lake. C. Close up showing the black welded scoria of 1668/1702 CE overlain by lahar and mass flow deposits ascribed to a 1903 CE eruption.

detailed study. In addition, three pumice samples from each of the deposits ascribed to the 1668/1702 and 1903 CE events.

All pumices were thoroughly rinsed with deionized water in an ultrasonic bath for 30 min to remove impurities, and then dried in an oven for 24 h. Each sample was divided into three portions, which were then prepared for thin-section, whole rock major analyses and epoxy mounts of mineral and glass for microanalysis. 18 polished thin-sections from two mixed pumices, eight ME and eight BGM pumices (including those from 1668/1702 and 1903 deposits) were subject to petrographic analysis. Whole-rock major element concentrations were measured using X-ray fluorescence spectrometer 2100 at the National Research Center for Geoanalysis, Chinese Academy of Geological Sciences. Analytical methods and standards have been documented in Part 28 of 'Methods for chemical analysis of silicate rocks' by National Standardization Technical committee of Land and Resources (Supplementary Table S2). Samples of pumice for microanalysis were crushed

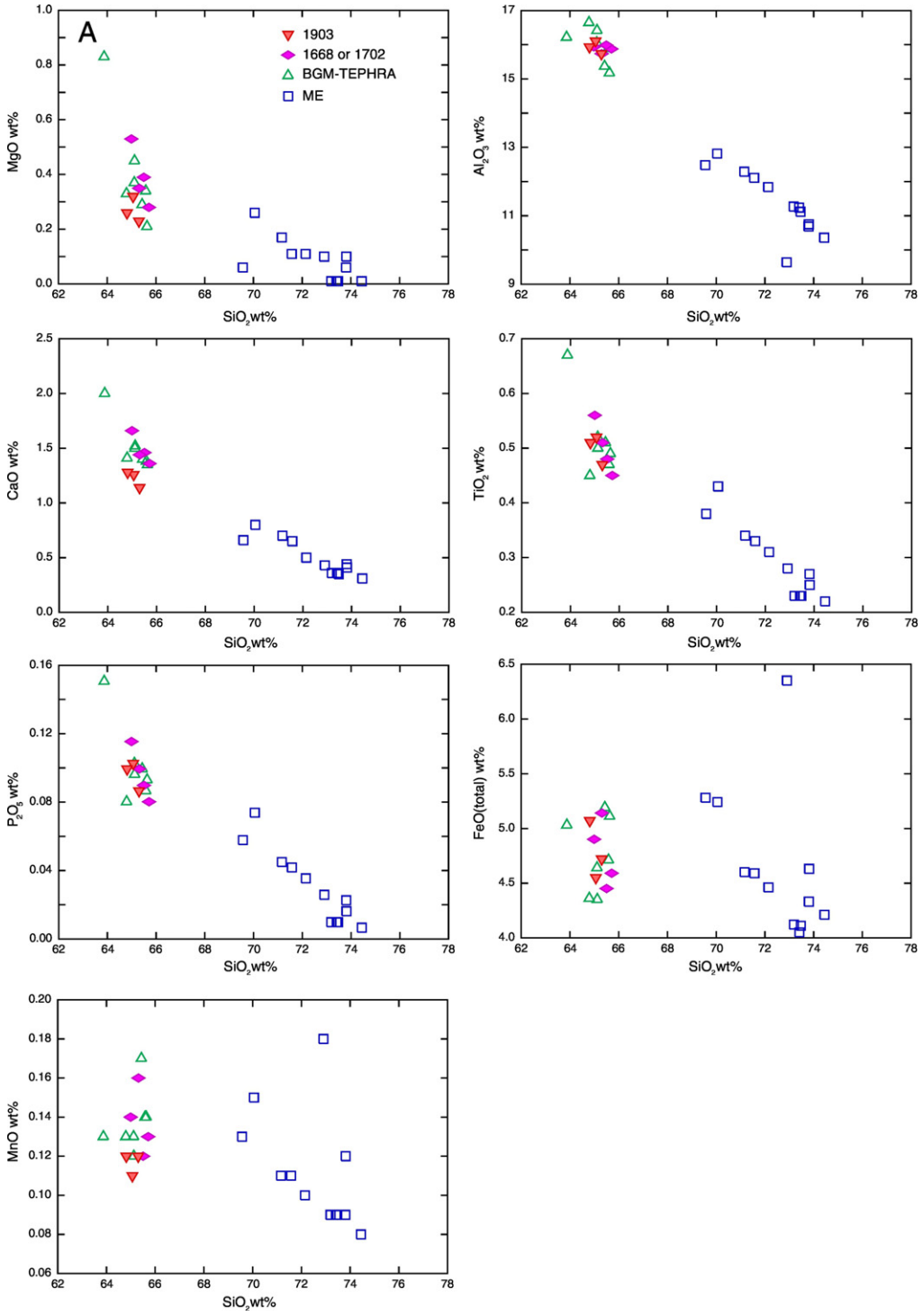

Fig. 6. Representative plots of whole-rock major and trace element data from the ME/BGM, 1668/1702 CE BGM, and 1903 CE deposits at and around Changbaishan in China. A. Whole rock major element Harker variation diagrams B. Whole rock trace element Harker and element-element variation diagrams. These show broad correlations with differentiation in the major elements except FeO and MnO, that are not supported in the trace elements. The compositional gap between the trachytes and comendites is clear as is the similarity in the ME/BGM tephra, the 1668/1702 CE BGM, and 1903 CE lithologies. The data are archived in Supplementary File S2 whole rock of major and trace elements. Symbols as in Fig. 2.

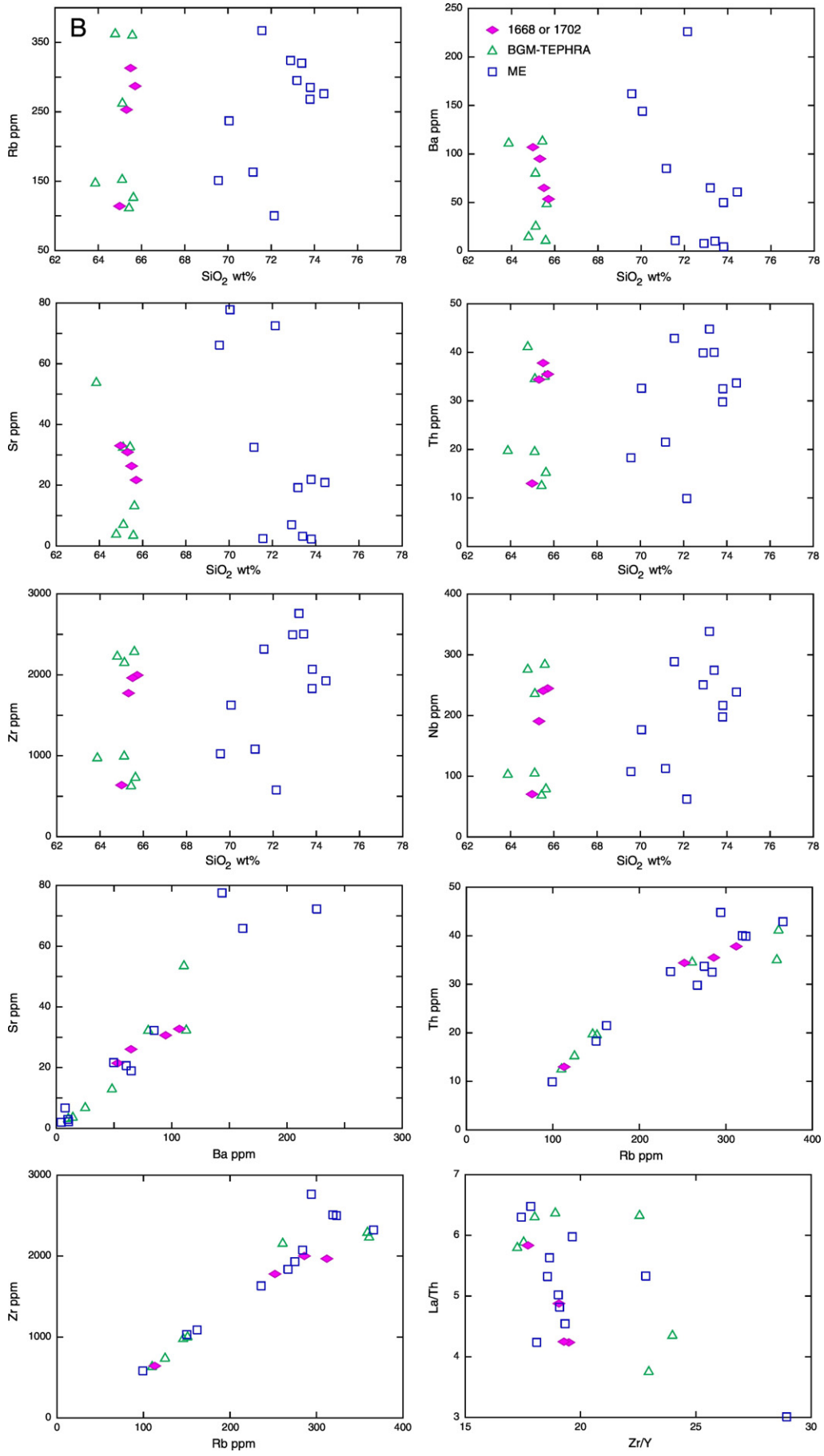

Fig. 6 (*continued*).

and sieved into different sizes, and then large glass shards of 63–300 μm and pyroxene were picked, mounted in epoxy, and polished. Where possible glass from different phases of mixed pumices were separated based on their color and then embedded in epoxy mounts and polished.

Major element compositions of 181 glass shards and 242 pyroxenes were determined by Electron Microprobe Analysis (EMPA) using a Cameca SX-100 electron microprobe at Oregon State University (OSU) with an accelerating voltage of 15 kV and an electron beam of 30 nA. Beam diameters were 5 um for glass and pyroxene analysis. In glass, Na and K were analyzed first and a zero intercept procedure was used to minimize any impact of alkali loss. Trace elements of 247 glass shards and 129 pyroxenes on the same mount measured by EPMA were also analyzed by LA-ICP-MS in the W.M Keck Collaboratory for Plasma Spectrometry at Oregon State University using a NewWave DUV 193 μm ArF

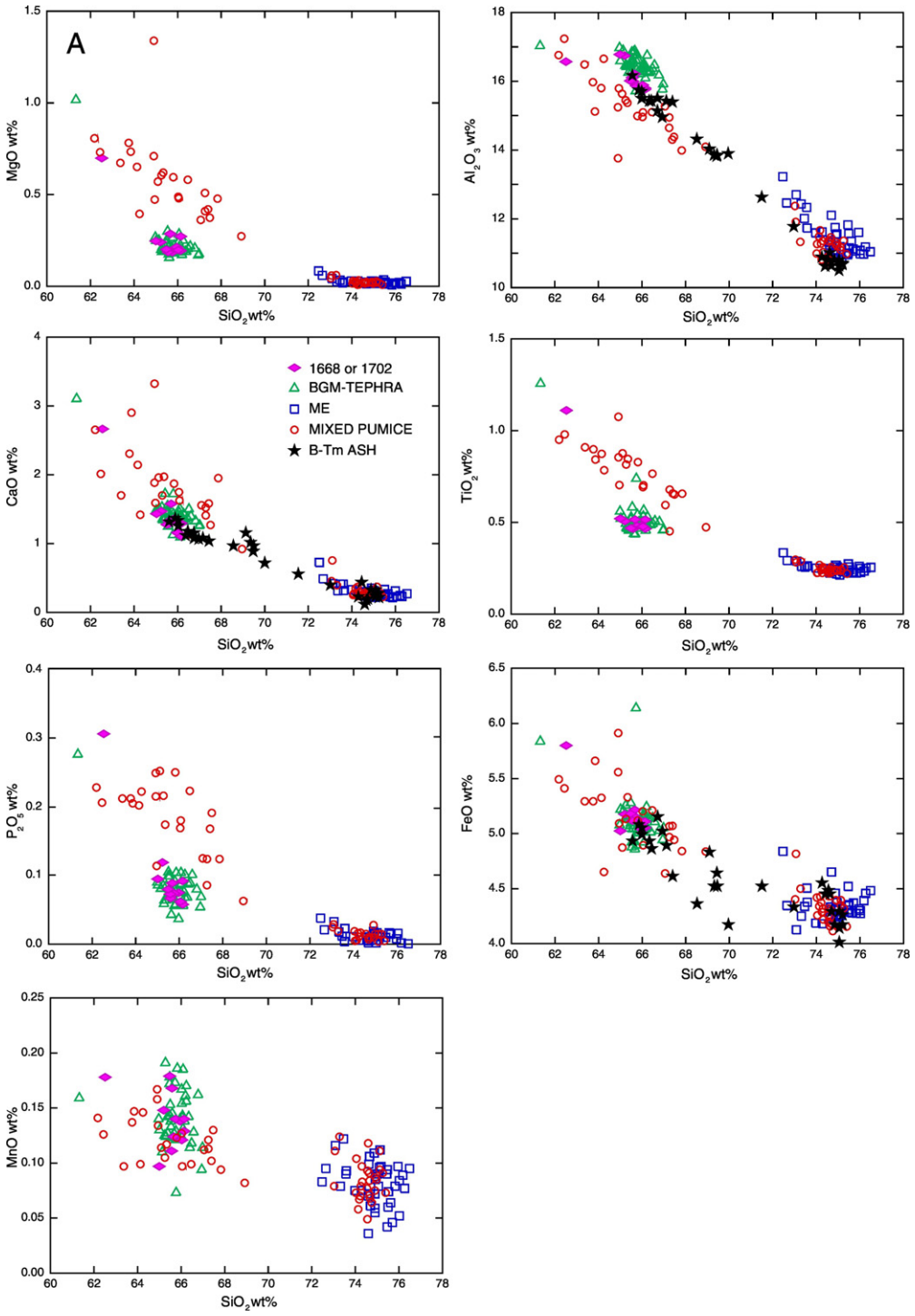

Fig. 7. Representative plots of matrix glass major and trace element data form juvenile clasts from ME/BGM, 1668/1702 CE BGM, and 1903 CE deposits at and around Changbaishan in China. A. Major element Harker variation diagrams. Data from the B-Tm ash from Ichinomegata maar, Japan (Okuno et al., 2011) is also plotted. B. Trace element Harker and element-element variation diagrams. These show broad correlations with differentiation in the major elements, and are supported in the trace elements, indicating the matrix glasses record a liquid line of descent. The compositional gap between the trachytes and comendites is clear as is the similarity in the ME/BGM tephra, the 1668/1702 CE BGM, and 1903 CE lithologies. The B-Tm glass shard data overlap very strongly with both the trachytes and the comendites but also extend into the compositional gap along with a few shards from the mixed pumices suggesting that some shards represent hybrid compositions. The data are archived in Supplementary Files S3a and S3b.

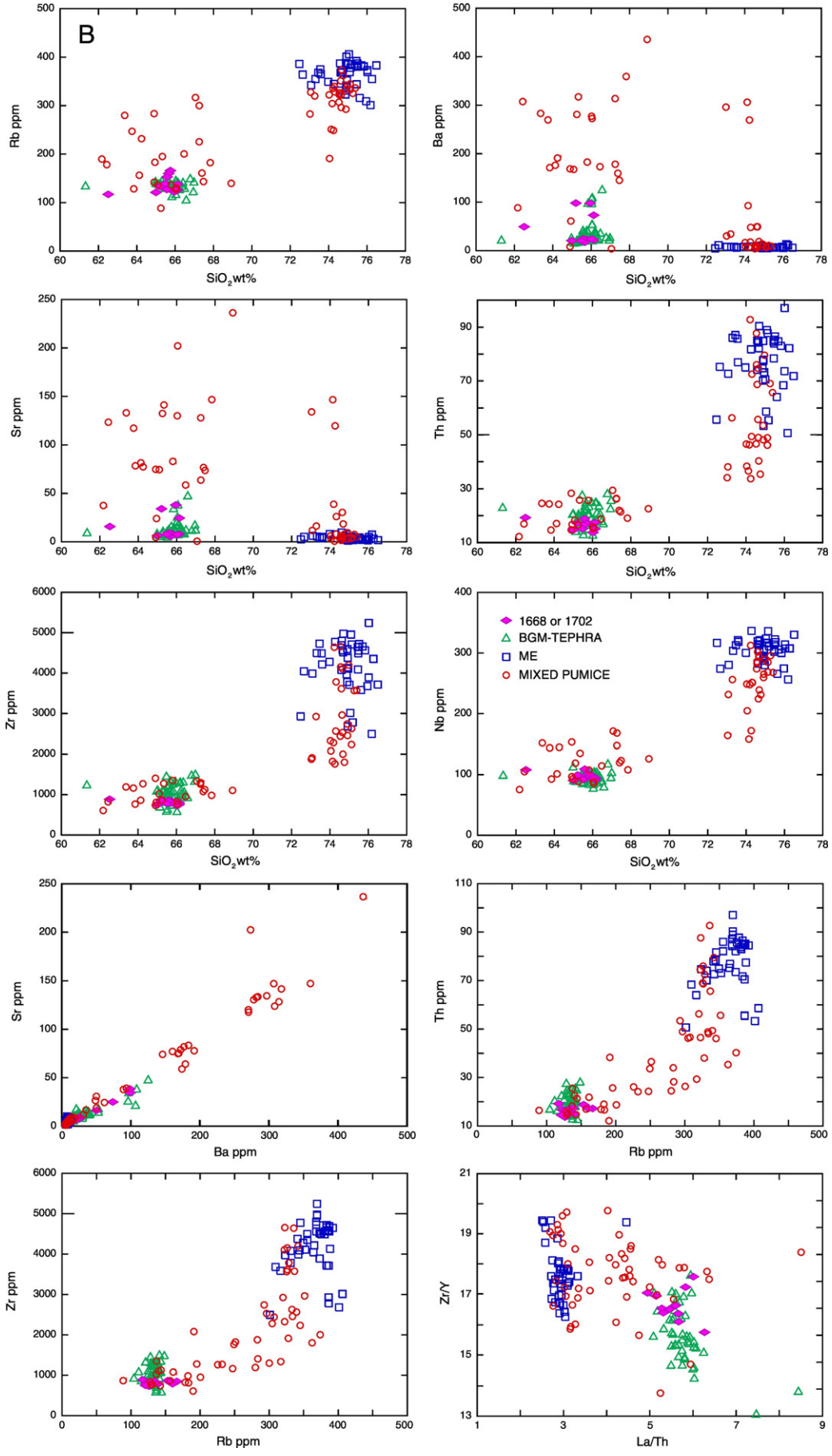

Fig. 7 (*continued*).

Excimer laser and VGPQ ExCell Quadrupole ICP-MS following techniques outlined in Kent et al. (2004). Laser ablation spot size was 50 μm for glass shard analysis and 60 μm for pyroxene analysis. Analytical methods for major and trace element analysis by the OSU LA-ICP-MS have been documented in the literature (e.g., Salisbury et al., 2012).

4. The link between the <1000 yr trachytes and the comendites

Key to resolving the debate over the post-ME eruptions is demonstrating that all the recent deposits at Tianchi are part of a single ME-BGM trachyte-comendite eruption. Below we present our field and petrochemical observations that inform this debate.

4.1. Field observations

The Tianwenfeng (T in Fig. 1) section located on the northern wall of Tianchi caldera clearly reveals the stratigraphy of the most recent eruptions of Changbaishan (Fig. 3). Here, the uppermost sequence clearly shows the black trachytic BGM tephra lying directly on the grey comenditic pumice of the ME without a depositional break (Fig. 3A–C). Away from the caldera rim, the relationship between the BGM and ME is largely obscured by forest and can only fully be revealed in river valleys or by trenching. Two of the most revealing sites are at Yuanchi and Dongfang (locations Y and D respectively on Figs. 1; 3B,C).

At Yuanchi, 28 km to east of the caldera, the comendite fall deposit of the ME is 45 cm thick, well sorted and is normally graded with maximum clast size of 5 cm at the bottom to ~0.1 cm on the top. Here, the internally-bedded trachytic scoria fall of the BGM lies directly on the ME without any traces of reworking or soil development (Fig. 3B). At Dongfang, 27 km to the northeast of Tianchi caldera, the BGM scoria fall directly overlies a co-ignimbrite ash layer that is the uppermost layer of the ME ignimbrite in this location (Fig. 3C). The contact relations seen at Tianwanfeng, Yuanchi, and Dongfang indicate there was no significant hiatus between the ME and BGM tephra deposition, and these three locations are representative of those we have seen at many other locations throughout this region (Fig. 1). If a 1668/1702 CE age for the BGM is correct, in this environment any such hiatus between eruptions would result in a significant unconformity or soil development. However, only at Dongfang is there any evidence of a break, where co-ignimbrite ash was deposited between the ME and BGM. Otherwise there is no break. Another key observation is that while the ME and BGM deposits are dominated by pumice of comendite and trachyte composition respectively, mingled comendite-trachyte or trachyte-comendite pumices (Fig. 3D) are found as a minor but ubiquitous component of both these tephra deposits. These attest to physical mixing between coexisting trachyte and comendite magma during the ME and BGM.

Deposits attributed to the 1668/1702 CE around the caldera are isolated outcrops that lie on ME comendite (Fig. 4). These locations are all within the mapped extent of the BGM fall deposits and given that they overlie ME comendite with no evidence of a break between the two, we hypothesize that these are part of the ME/BGM eruption.

The putative 1903 CE deposits are located on the shore of the Tianchi Lake in places directly overlying the 1668/1702 CE deposits (Fig. 5). In the historic record, this event is described as some sort of flare-up (See Supplementary File S1), which has been translated to a phreatomagmatic eruption by Wei et al. (2013). However, the deposits on the lakeshore attributed to the 1903 CE event, consist of coarse-fines-depleted, loose, chaotic to thinly bedded, heterogeneous deposits of pumice, scoria, lithic fragment, sand and soil, with the lowest parts dominated by sandy material. No evidence of any primary pyroclastic bedding, bomb sags or welded spatter as might be expected from a proximal phreatomagmatic deposit was found. We interpret this as slumped, mass wasted, and laharic deposits derived from the ME deposits on the caldera wall, that have been reworked by water.

In summary, field observations indicate that deposits attributed to a 1668/1702 CE are equivalent to the BGM trachyte that is the late stage of the ME. Deposits ascribed to the 1903 CE event are slumped/mass wasted deposits of ME deposits from the caldera walls and then reworked by the lake. We test these interpretations further below.

4.2. Petrology and geochemistry

The dominant ME pumices exhibit a range of 75–76% SiO_2 classifying as comendite (Fig. 2). They are moderately peralkaline with agpaitic indices ranging from1.2 to 1.4. The dominant BGM scoria is also quite limited in composition ranging from ~64–66% SiO_2 classifying as trachyte with agpaitic indices ranging from 0.9 to 1.05. A clear compositional gap of almost 10% SiO_2 separates these two end-member bulk compositions. Mingled pumices range from 70 to 75% SiO_2, only partially filling the compositional gap. The trachytic and comenditic end member compositions are typical of those erupted throughout the last million years of Tianchi volcano (Liu et al., 1998). Samples from the putative 1668/1702, and 1903 CE deposits are indistinguishable from the BGM trachytes.

The comenditic pumice of the ME tephra is leucocratic, typically white or grey, vesicular (35 to 50%) with slender glass walls. It is phenocryst-poor with ~5–8 vol% crystals of anorthoclase to Na-sanidine (~90%), Hedenbergite (~5%), fayalitic olivine (~3%), and quartz (~2%). In contrast, the BGM trachytic pumice is melanocratic, black or dark yellow, vesicular (max 30%). Crystal contents are ~30% by volume and consist of sanidine (~80%), pyroxene (~10%), olivine (~5%), ilmenite (~3%), and quartz (~2%). A distinct feature of the feldspar and pyroxene phenocrysts in the BGM scoria is the pervasive development of melt-inclusions, disequilbrium textures and evidence of resorption. These features are again seen in the 1668/1702, and 1903 CE trachytic pumice. The mixed pumice consists of variably interlaced comendite and trachyte (Fig. 3D). The grey comendite portions are relatively phenocryst-poor, with slender glass walls, while the black trachytic selvages are rich in large phenocrysts or contain polycrystalline aggregates and thick glass walls.

The bulk rock compositions display weakly linear trends on Harker diagrams with minor inflexions suggesting a change in fractionation assemblage at about 66% SiO_2 consistent with the mineral assemblages seen in the rocks (Fig. 6A). The reduction in alkalis from trachyte to comendite (Fig. 2) is probably the result of a large proportion of alkali feldspar fractionation in the minimum melt (rhyolitic) compositions. However, FeO and MnO show no clear trend with SiO_2 probably due to accumulation of Fe-Ti oxides. Harker diagrams of trace elements similarly show no systematic trends and although compatible and incompatible elements are correlated respectively, there are no correlation between the two groups (Fig. 6B). In fact the range for most trace elements is the same for the comendites and the trachytes. When combined with the evidence for microscopic mingling in most of the rocks, we conclude that the individual bulk rock compositions are not pure liquid compositions and we interpret any trends with caution. The 1668/1702 and 1903 CE samples all plot within the main BGM field.

Matrix glass compositions are representative of liquid compositions and display coherent trends from trachyandesite through trachyte to comendite. The presence of glass selvedges more mafic than the host bulk rock compositions in both the ME comendite and BGM trachyte and more silicic than the host BGM trachyte attests to microscopic mingling of BGM trachyte with ME comendite as well as implicating a role for more mafic compositions in the Changbaishan magma system. All these melts define a liquid line of descent in which the comendites can be produced by fractionation of olivine, plagioclase, and ilmenite from trachytic or trachyandesite melts (Fig. 7A). Again the 1668/1702 CE pumices are indistinguishable from the BGM trachyte. Note that no 1903 CE samples were used for microanalysis once it was clear that these were reworked deposits and there the bulk rock compositions were identical to the BGM.

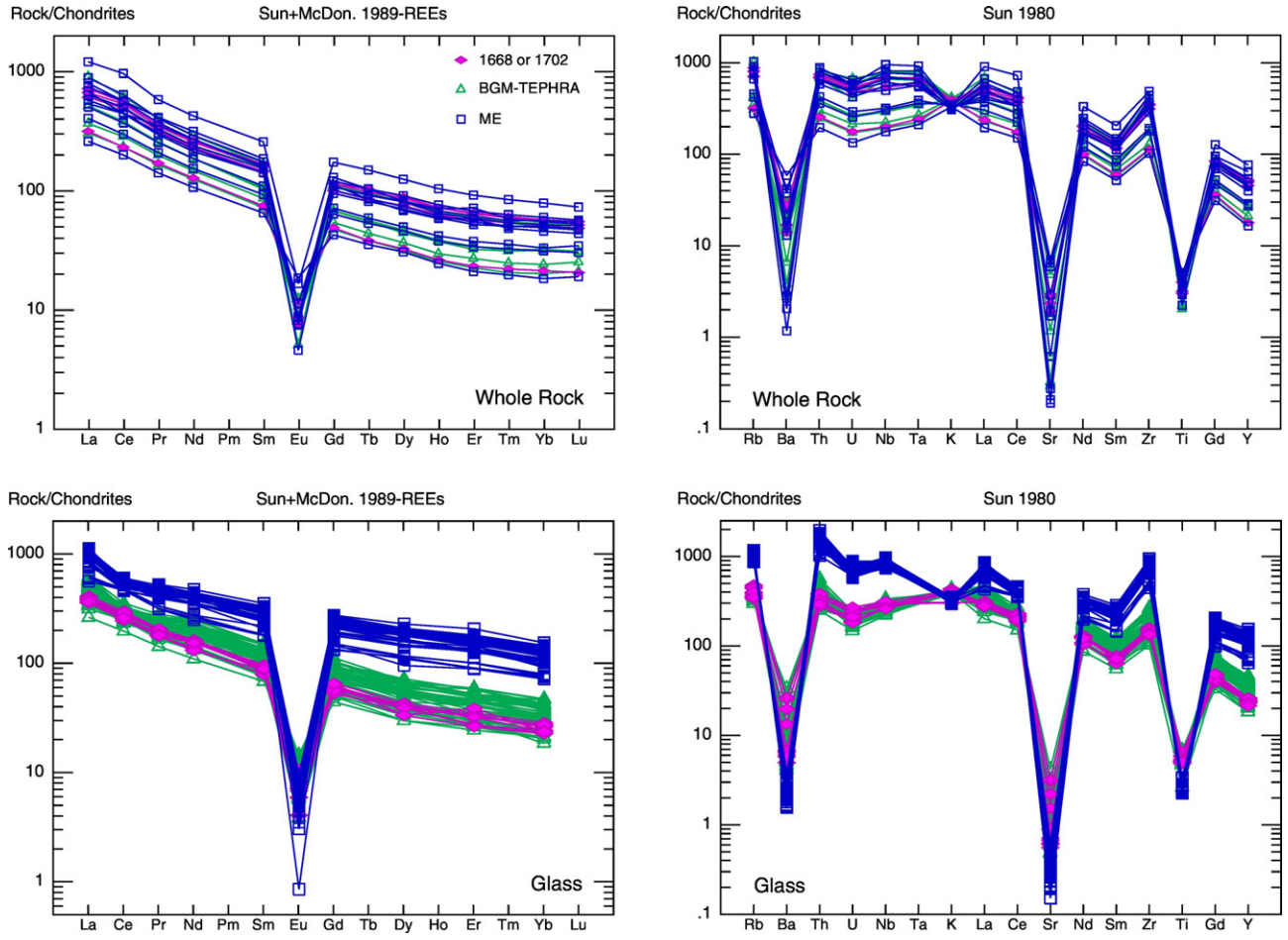

Fig. 8. Multi-element "spider" of rare-earth (left) and trace elements (right) for whole rock (upper) and glass shards (lower). Symbols as used previously. REE are normalized to Sun and McDonough (1989) and the full trace element data to Sun (1980). These plots also re-iterate the bimodality of the juvenile lithologies are Changbaishan, and the compositional overlap between the ME trachytes and those attributed to 1668/1702 CE. The full data set is archived in Supplementary files S2 and S3b.

Like in the bulk samples, a compositional gap is seen, this time from 67% to 72.5% SiO_2, even when matrix glass from mixed pumices is included. The smaller compositional gap is consistent with the macroscopic evidence of mingling of trachyte melt in the comendite pumice and vice versa. The glass compositions also record trace quantities of trachyandesite melt within the trachytic BGM pumices. A hint of two trends is evident; the trachytic and trachy-andesitic glass in mingled pumices showing elevated MgO, P_2O_5, TiO_2, and lower Al_2O_3 Incompatible and compatible trace elements of glass shards (Figs. 7B, 8) confirm the mingling of these magmas, but elevated Sr, Ba, and to a lesser extent Rb in mixed pumice glasses suggest inadvertent analysis of portions of feldspar during laser analysis of fine-scale mingled glass. Nonetheless systematic differences in incompatible elements Zr, Nb, Th, La, and Y between the ME and BGM are clear with no overlap, with the former being

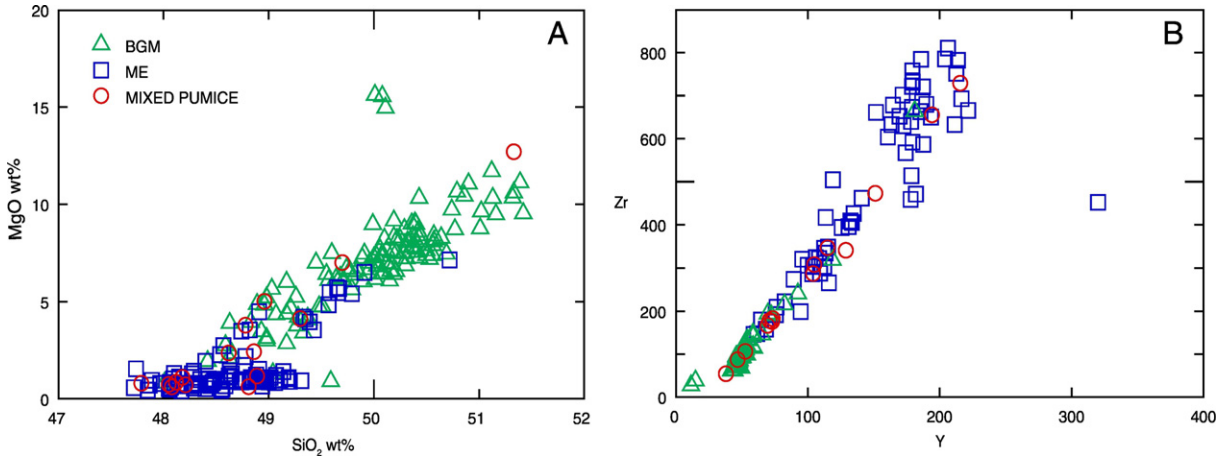

Fig. 9. Plots of MgO and Zr from pyroxene phenocrysts from the ME comendite and BGM trachyte clasts and from mixed pumices. These two plots are representative for the entire data set. While pyroxenes from the trachyte and comendite are distinct they define a general differentiation trend. The mixed pumices contain pyroxenes from both the ME eruption end members and mutual exchange of phenocrysts between the comendite and trachyte is also clear. Full data sets are given in Supplementary files S4a and S4b.

elevated in these elements. Glasses from the mixed pumice overlap with and bridge the gap between the groups (Fig. 7B). The 1668/1702 CE samples all plot within the main BGM field.

Trace element and Rare Earth Element (REE) systematics largely support these observations (Fig. 8). Bulk compositions show that the ME pumices have the most elevated REE contents but there is significant overlap with those of the BGM pumices that generally have lower REE. Trace elements show no clear distinction and ME and BGM bulk compositions overlap significantly. A clear separation of the two is seen in the glass compositions however, with the ME showing higher REE and incompatible elements, and lower compatible elements (Ba, Sr, Ti) compared to the BGM glass. In these cases 1668/1702 CE samples all plot within the BGM pumices.

Major and trace elements of pyroxene relay the same story as the matrix glass. The pyroxenes in the ME comendite and BGM trachytes as well as 1668/1702 CE pumices define distinct groups along a continuum with some small overlap (Fig. 9). The hedenbergites in the ME comendite are enriched in MgO and FeO and have higher Zr and Y whereas those in trachytes are enriched in CaO and have lower Zr and Y. The pyroxene data from mixed pumice extend across both groups.

5. Discussion

Field relations, petrography, bulk and micro-scale chemistry indicate a Millennium-Baguamiao (ME-BGM) tephra sequence deposited during a single climactic eruption that records physical mixing of trachytic and comenditic magmas. These data also indicate that trachytes attributed to eruptions in 1668/1702 CE are outcrops of the BGM tephra, and the 1903 CE deposits are reworked deposits of the ME-BGM sequence on the caldera wall. Below we integrate these observations with previous

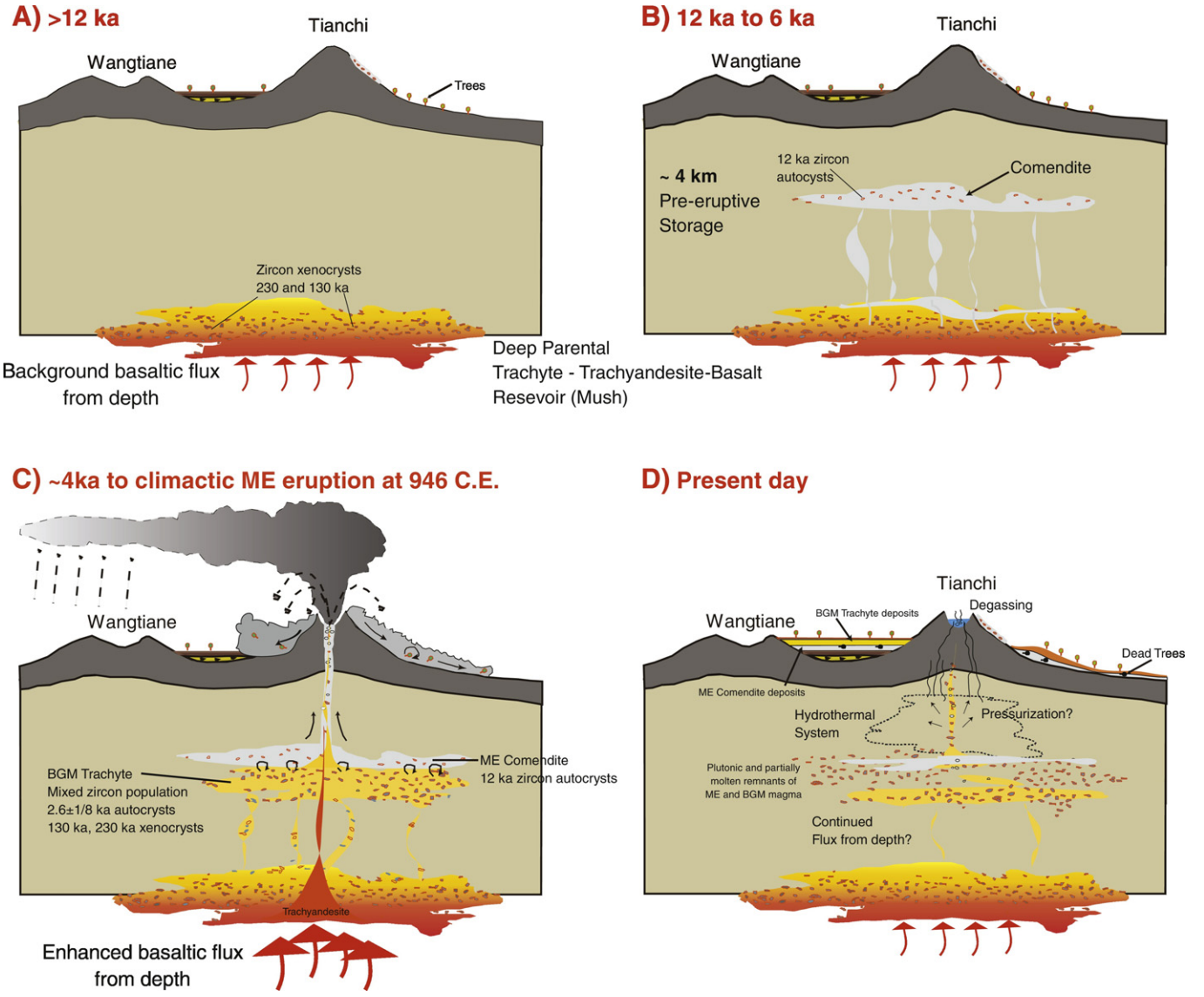

Fig. 10. Magma dynamics of the Millennium Eruption. A. Steady-state magmatic system maintained by a background parental basaltic flux. Pre-12 ka a parental trachyte, not that of the BGM per se, begins to accumulate through fractionation from basaltic. The heterogeneous age populations of zircons from the BGM scoria implicates a long-lived mush that was oscillating in and out of zircon saturation for a significant period of time (>200 ka). B. As this trachytic mush zone evolves derivative comendite melts started to form, fractionate and accumulate at shallow levels at least ~ 12 ka (zircon data of Zou et al., 2014) till at least 6 ka based on Ra/Th data of Ramos et al. (2016). C. ~4–1 ka Ra/Th model ages suggest that ~2.5 to 1.5 ka, trachyte accumulates separately from the comendite, Zircon autocrysts form in the trachyte. Close to 946 CE and enhanced flux of parental basalt into the deep mush releases a pulse of trachyandesite. This interacts with the BGM trachyte carrying crystal cargo with multi-age populations of zircons upwards. Mixing and mingling with the ME comendite results in overturn and triggering of the climactic Millennium eruption, magma mixing and resulting in the comendite-trachyte sequence. Pyroclastic deposits inundate and incorporate pre-existing forests. D. Present day. Return to background basaltic flux that maintains the system in a melt-present state. Continued unrest at Changbaishan-Tianchi suggests that remnants of the trachyte-comendite magma system may still be in a partially molten state and maybe kept active through thermal flux form depth. Passive degassing and pressurization of the conduit or pressurization of a sub-caldera hydrothermal system may explain the intermittent degassing, seismicity and deformation.

work on the Changbaishan-Tianchi system to refine the model for the eruption and the magma dynamics that led to it.

5.1. An integrated comendite-trachyte Millennium eruption

Further support for a single ME comes from that fact that the BGM trachyte has the same Ra/Th (age corrected) model age as the 1668, 1702, and 1903 CE trachyte samples (Ramos et al., 2016). The weight of evidence then points to a simple volcanic history where the last eruption of Tianchi caldera was the comendite-trachyte ME-BGM eruption. We include all these deposits in the ME eruption, thus supporting and extending the previous assertions of Dunlap (1996), Tokui (1989) and Horn and Schmincke (2000) and providing continuity with established nomenclature.

The chemostratigraphy clearly reveals dominant comendite transitioning to mingled comendite-trachyte, to trachyte with mingled comendite and trachyandesite later in the eruption. Distal ash deposits in Japan support this. The Baitoushan-Tomakomai (B-Tm) tephra, which is the designation for the distal ash deposits of the ME eruption in Japan, is a well-known stratigraphic marker in the Japan Sea and north of Japan (Machida and Arai, 1983; Oppenheimer et al., 2017). Okuno et al. (2011) identified ~2 mm of B-Tm tephra in a 37 m long sediment core in Ichinomegata Lake (abbreviated as I on Fig. 1). The major elements of 35 glass shards of B-Tm show compositions corresponding to the respective compositions of the ME and BGM matrix glass compositions (Fig. 7A; Al_2O_3, CaO, and FeO), confirming that both comendite and trachyte ash shards were contemporaneously deposited. Our work further verifies the correlation of the B-Tm ash with the ME eruption and supports its status as a key chronostratigraphic marker (e.g. Oppenheimer et al., 2017).

5.2. Magma dynamics of the Millennium eruption

Close association of comendite and trachytic magmas is a consistent feature of the recent history of Tianchi volcano. Eruptions throughout the last 100 ka at Tianchi, and maybe as far back as 1 Ma, show regular alternations of trachyte and comendite (Liu et al., 1998). This consistent compositional history suggests that conditions for interaction between comendite and trachyte are a feature of Tianchi volcano and probably play a part in the major explosive eruptions there. Thus the magma dynamics of the ME bears further consideration. Based on available geochronology and our new volcanological framework for a single eruption we provide a possible model for the magma dynamics leading to the ME (Fig. 10).

Prior to the ME, two distinct magmas, a comendite and a trachyte, must have existed under Tianchi, and mixed prior to or during the eruption. The comendite can be derived from trachytic magmas like that of the BGM by fractional crystallization, but the large compositional gap suggests that once formed the comendite melts segregated and evolved separately from the trachytes. Starting with a trachytic magma similar to that of the BGM, more evolved comendite could be produced by feldspar, olivine and ilmenite fractionation. We note that based on melt inclusion chemistry (Horn and Schmincke, 2000) suggest that a less evolved trachyte, not that of the BGM per se, was the parent to the ME comendite. This is consistent with the findings of Dunlap (1996), although in that work a trachytic parent to the ME comendite and a later hybrid latite is posited. Our data is consistent with this except that rather than latite we see selvedges of trachyandesite. The distinction is small and can be explained by local differences in glass composition in response to local variations in crystallizing assemblage and crystal content. Ultimately we also support a role for more mafic magmas at Tianchi, and surmise that the whole system is driven by basaltic input from depth (Fig. 10). Further insight into the magma dynamics comes from recent U-series age data (Ramos et al., 2016) and zircon U-Th age systematics (Zou et al., 2014).

Zou et al. (2014) obtained a fairly uniform set of zircon U-Th ages of 12.2 ± 1.1 ka, from the ME pumice but a multimodal population with age modes of 2.6 ± 1.8 ka, 130 ± 10 ka, and >230 ka from the BGM scoria, with the youngest population reflecting the most recent history of the trachyte. Thus although the two magmas maybe consanguineous, they were not contemporaneous and could not have shared the same magma reservoir. The heterogeneous age populations from the BGM scoria suggest a long history of incremental assembly by pulses of magmatism (e.g. Coleman et al., 2004; Ruprecht and Bachmann, 2010; Farina et al., 2012) and consistent with the high crystallinity, coarse texture and the prevalence of disequilibrium textures. This connotes a long-lived mush beneath Tianchi that was oscillating in and out of zircon saturation for a significant period of time (>200 ka).

As this trachytic mush zone evolved, the U-Th in zircon data of Zou et al. (2014), suggests that less dense comendite fractionated and collected at shallow levels at least ~ 12 ka and Ra/Th model ages suggest that crystallization of the ME comendite continued at least till ~6 ka (Ramos et al., 2016). These data indicate an extended period of comendite accumulation and residence prior to the ME.

Subsequent accumulation of the BGM trachyte, derived from the same parental mush as the comendite, occurred ~4–1 ka (2.6 ± 1.8 ka) as indicated by the U-Th in zircon data of Zou et al. (2014). Ra/Th model ages suggest that trachyte melts continued to form and accumulate from 2.5 to 1.5 ka, remaining separate from the comendite (Ramos et al., 2016). The incremental accumulation of the trachyte beneath or adjacent to, but separate from, the comendite may have sustained the latter in a mushy state, with the thermal impact of a background basaltic flux maintaining the system, as has been posited for numerous long-lived magmatic systems (e.g. Hildreth and Wilson, 2007).

Approximately 1 ka, the long term stable association of trachyte and comendite was disrupted culminating in the ME. The climactic eruption may have been triggered by a combination of magma mixing and overturn of the comendite-trachyte sequence. Trachyandesite apparently plays a role. Interaction between parental basalts and the deep mush could have released hybrid trachyandesite (or latite; Dunlap, 1996), that then invaded and mingled with the trachyte (BGM in our framework) and instigated further mixing, mingling, that triggered the climactic eruption (Fig. 10c). This scenario is consistent with the Ra/Th model ages of Ramos et al. (2016) who find that the latite/trachyandesite has corrected model ages concordant with the ME comendite and BGM trachyte. We speculate that this disruptive sequence of events may have been fueled by an enhanced pulse of basaltic input into the basal trachytic mush that disrupted a steady state magma system (Fig. 10c).

Macroscopic and microscopic textural and chemical evidence shows that mingling on the crystal scale to mm occurred. Distinct compositional ranges of the phenocrysts of the comendite and trachyte respectively allow identification of mutually exchanged xenocrysts. The distinct matrix glass on the sub-millimeter scale and the lack of evidence for equilibration suggests a very short time scale for contact between the magmas before freezing. Since diffusivities of major elements are on the order of 10-12m2s-1 (Liang et al., 1996), using $t \sim x / D$, we can estimate that the amount of time (t) needed to diffusively equilibrate length scales (x) of 1 mm is on the order of 10 days. However, thermal diffusion, which typically proceeds at rates orders of magnitude faster (10-6m2s-1), would result in freezing of the melts in a matter of seconds. This first order calculation helps us understand why no hybridization took place between the comendite, trachyte, and trachyandesite; even at the mm scale chemical equilibration was too slow to compete with freezing of the melts. This leads us to the conclusion that recharge probably triggered the ME eruption and intimate mingling of the magmas had to have happened during the eruption probably in the conduit.

6. Conclusions

The trachytic BGM tephra at Changbaishan-Tianchi volcano is the late stage of the 946 CE "Millennium" eruption, and is not tephra deposited during putative eruptions in 1668/1702 or 1903 CE for which we find no physical evidence. Thus, the great "Millennium" eruption is now revised to include an early comendite and late trachyte stage. Hazard assessments of Changbaishan that have emphasized a "Baguamiao" explosive eruption ca. 1668/1702 and a later eruption in 1903, need to be reconsidered. Our findings also explain the bimodal compositions of glass shards in the important B-Tm tephra that forms an important stratigraphic marker, and further supports the correlation of the B-Tm ash with the ME.

Multiscale textural and chemical characteristics indicate mingling of trachytic and comenditic magma that had been accumulating and evolving separately under Tianchi volcano millennia before the climactic eruption. A role for deeper recharge by more mafic magmas in setting these processes in motion is suggested by rare trachyandesite compositions. The lack of chemical homogenization despite mingling on the sub-millimeter scale indicates that trachyte-comendite mixing had to have happened in a few hours most likely during eruption. The close association of comendite-trachyte in the ME appears to be a long term condition at Tianchi volcano over at least the last 100 ka. This enhances opportunities for catastrophic interaction of these magmas to fuel explosive activity at Tianchi.

The sequence of events that culminated in the climactic ME, requires a major change in the magmatic system at Tianchi involving more mafic trachyte. This implicates enhanced basaltic flux into the upper crustal system beneath Tianchi as the trigger for these events and eventual eruption. In this respect the ME of Changbaishan-Tianchi is similar to many major historic eruptions that have been triggered by magma mixing/recharge (Sparks and Sigurdsson, 1977; Kress, 1997; de Silva et al., 2008; Tepley et al., 2013). Such recharge events may be revealed in gas emissions, deformation, and seismicity at Tianchi (e.g. Pinatubo - Kress, 1997) and these should be regularly monitored. The evidence for a protracted history of comendite-trachyte magma dynamics at Tianchi needs to be considered in interpreting signals of current unrest at one of Asia's most dangerous volcanoes.

Supplementary files: complete data tables for bulk and micro-analytical geochemistry. Supplementary data associated with this article can be found in the online version, at http://dx.doi.org/10.1016/j.jvolgeores.2017.05.029.

Acknowledgements

This research was supported by the China National Science Foundation (41302267) and the Special Projects of the Institute of Geology, CEA (IGCEA1505). Bo Pan thanks the China Scholarship Council for the opportunity for the study visit to Oregon State University. Frank Tepley provided assistance with EMPA, and Adam J.R. Kent provided assistance with LA-ICP-MS. We thank the Changbaishan National Park and Changbaishan Volcano Observation Station for assistance during fieldwork over many years. The insightful comments from two knowledgeable journal reviewers and the editorial handling by Dr Kelly Russell are much appreciated. These improved this contribution in substance and clarity.

References

Brown, S.K., Crosweller, H.S., Sparks, R.S.J., Cottrell, E., Deligne, N.I., Guerrero, N.O., Hobbs, L., Kiyosugi, K., Loughlin, S.C., Siebert, L., Takarada, S., 2015. Characterisation of the Quaternary eruption record: analysis of the Large Magnitude Explosive Volcanic Eruptions (LaMEVE) database. J. Appl. Volcanol. 3, 22.

Chun, J.H., Cheong, D., Lee, Y.J., Kwon, Y.I., Kim, B.C., 2006. Stratigraphic implications as a time marker of the B-J tephra erupted from Baegdusan volcano discovered in the marine cores of the East Sea/Japan Sea during the late Pleistocene. J. Geol. Soc. Korea 42, 31–42.

Coleman, D.S., Gray, W., Glazner, A.F., 2004. Rethinking the emplacement and evolution of zoned plutons: geochronologic evidence for incremental assembly of the Tuolumne Intrusive Suite, California. Geology 32, 433–436.

Crosweller, H.S., Arora, B., Brown, S.K., Cottrell, E., Deligne, N.I., Guerrero, N.O., Hobbs, L., Kiyosugi, K., Loughlin, S.C., Lowndes, J., Nayembil, M., Siebert, L., Sparks, R.S.J., Takarada, S., Venzke, E., 2012. Global database on large magnitude explosive volcanic eruptions (LaMEVE). J. Appl. Volcanol. 1, 1–13.

Dunlap, C.E., 1996. Physical, Chemical, and Temporal Relations Among Products of the 11th Century Eruption of Baitoushan, China/North Korea [Ph.D. Thesis]. University of California, Santa Cruz (104 pp.).

Fan, Q.C., 2008. History and evolution of Changbaishan volcano. Resources Survey and Environment. vol. 29, pp. 196–203.

Fan, Q.C., Sui, J.L., Wang, T.H., Li, N., Sun, Q., 2007. History of volcanic activity, magma evolution and eruptive mechanisms of the Changbai volcanic province. Geol. J. China Univ. 13, 175–190.

Farina, F., Stevens, G., Villaros, A., 2012. Multi-batch, incremental assembly of a dynamic magma chamber: the case of the Peninsula pluton granite (Cape Granite Suite, South Africa). Mineral. Petrol. 106 (3), 193–216 10.1007/s00710-012-0224-8.

Hildreth, W., Wilson, C.J.N., 2007. Compositional zoning of the Bishop Tuff. J. Petrol. 48 (5), 951–999.

Horn, H., Schmincke, H.U., 2000. Volatile emission during the eruption of Baitoushan volcano (China/North Korea) ca. 969 AD. Bull. Volcanol. 62, 537–555.

Jin, D.C., Cui, Z.X., 1999. A study of volcanic eruption in Tianchi volcano, Changbai Mountain recorded in historical documents. Geogr. Rev. 45, 304–307.

Kent, A.J.R., Stolper, E.M., Francis, D., Woodhead, J., Frei, R., Eiler, J., 2004. Mantle heterogeneity during the formation of the North Atlantic Igneous Province: Constraints from trace element and Sr-Nd-Os-O isotope systematics of Baffin Island Picrites. Geochem. Geophys. Geosyst 5. http://dx.doi.org/10.1029/2004GC000743 Q11004.

Kress, V., 1997. Magma mixing as a source for Pinatubo sulphur. Nature 389 (6651) 591–593. http://dx.doi.org/10.1038/39299.

Liang, Y., Richter, F.M., Davis, A.M., Watson, E.B., 1996. Diffusion in silicate melts: I. Self diffusion in CaO-Al2^{O}3^{-SiO}2 at 1500 °C and 1 GPa. Geochim. Cosmochim. Acta 60, 4353–4367.

Liu, R.X., Wei, H.Q., Li, J.T., 1998. The Recent Eruptions of Changbaishan Tianchi Volcano. Science Press, Beijing, China.

Machida, H., 1999. The stratigraphy, chronology and distribution of distal marker-tephras in and around Japan. Glob. Planet. Chang. 21, 71–94.

Machida, H., Arai, F., 1983. Extensive ash falls in and around the sea of Japan from large late quaternary eruptions. J. Volcanol. Geotherm. Res. 18, 151–164.

Nanayama, F., Satake, K., Furukawa, R., Shimokawa, K., Atwater, B.F., Shigeno, K., Yamaki, S., 2003. Unusually large earthquakes inferred from tsunami deposits along the Kurile trench. Nature 424, 660–663.

Okuno, M., Torii, M., Yamada, K., Shinozuka, Y., Danhara, T., Gotanda, K., Yonenobu, H., Yasuda, Y., 2011. Widespread tephras in sediments from lake Ichi-no-Megata in northern japan: their description, correlation and significance. Quat. Int. 246, 270–277.

Oppenheimer, C., 2011. Eruptions That Shook the World. Cambridge Univ, Press, Cambridge, U. K.

Oppenheimer, C., et al., 2017. Multi-proxy dating the 'Millennium' eruption of Changbaishan to late 946 CE. Quat. Sci. Rev. 158, 164–171.

Ramos, F.C., Heizler, M.T., Buettner, J.E., Gill, J.B., Wei, H.Q., Dimond, C.A., Scott, S.R., 2016. U-series and ^{40}Ar/^{39}Ar ages of Holocene volcanic rocks at Changbaishan volcano. China. Geology 44 (7), 511–514.

Ruprecht, P., Bachmann, O., 2010. Pre-eruptive reheating during magma mixing at Quizapu volcano and the implications for the explosiveness of silicic arc volcanoes. Geology 38, 919–922.

Salisbury, M.J., Patton, J.R., Kent, A.J.R., Goldfinger, C., Djadjadihardja, Y., Hanifa, U., 2012. Deep-sea ash layers reveal evidence for large, late Pleistocene and Holocene explosive activity from Sumatra. Indonesia. J. Volcanol. Geotherm. Res. 231-232, 61–71. http://dx.doi.org/10.1016/j.jvolgeores.2012.03.007.

Siebert, L., Simkin, T., Kimberley, P., 2010. Volcanoes of the World. University of California Press, Berkeley, CA (551 pp.).

de Silva, S., Salas, G., Schubring, S., 2008. Triggering explosive eruptions—the case for silicic magma recharge at Huaynaputina, southern Peru. Geology 36, 387–390.

Sparks, R.S.J., Sigurdsson, H., 1977. Magma mixing: a mechanism for triggering acid explosive eruptions. Nature 267, 315–318.

Stone, R., 2011. Vigil at North Korea's Mount Doom. Science 334, 1–5.

Stone, R., 2013. Sizing up a slumbering giant. Science 341, 1060–1061.

Sun, S.S., 1980. Lead isotopic study of young volcanic rocks from mid-ocean ridges, ocean islands and islandarcs. Philos. Trans. R. Soc. Lond. A297, 409–445.

Sun, S.S., McDonough, WF., 1989. Chemical and isotopic systematics of oceanic basalts: implications for mantle composition and processes. In: Saunders, AD, Norry, MJ (Eds.), Magmatism in the Ocean Basin. Geological Society Special Publication, pp. 313–345.

Tepley, F.J., De Silva, S., Salas, G., 2013. Magma dynamics and petrological evolution leading to the VEI 5 2000 BP eruption of El Misti volcano, Southern Peru. J. Petrol. 54, 2033–2065.

Tokui, Y., 1989. Volcanic eruptions and their effects on human activity in Hokkaido, Japan. Annals of Ochanomizu Geographical Society. vol. 30, pp. 27–33.

Wei, H.Q., Wang, Y., Jin, J.Y., Gao, L., Yun, S.H., Jin, B.L., 2007. Timescale and evolution of the intracontinental Tianchi volcanic shield and ignimbrite-forming eruption, Changbaishan, Northeast China. Lithos 96, 315–324.

Wei, H.Q., Liu, G.M., Gill, J., 2013. Review of eruption activity at Tianchi volcano, Changbaishan, northeast China: implications for possible future eruptions. Bull. Volcanol. 75, 705–719.

Xu, J.D., Liu, G.M., Wu, J.P., Ming, Y.H., Wang, Q.L., Cui, D.X., Shangguan, Z.G., Pan, B., Lin, X.D., Liu, J.Q., 2012. Recent unrest of Changbaishan volcano, northeast China: a precursor of future eruption? Geophys. Res. Lett. 39, L16305.

Xu, J.D., Pan, B., Liu, T.Z., Hajdas, I., Zhao, B., Yu, H.M., Liu, R.X., Zhao, P., 2013. Climatic impact of the Millennium eruption of Changbaishan volcano in China: new insights from high-precision radiocarbon wiggle-match dating. Geophys. Res. Lett. 40, 54–59.

Yu, H.M., Wu, J.P., Xu, J.D., Lin, C.Y., Shi, L.B., Chen, X.D., 2012. Microstructural characteristics of the Holocene pumice erupted from Changbaishan Tianchi volcano and their volcanological implications. J. Jilin Univ. (Earth Sci. Ed.) 42, 132–144.

Yun, S.H., 2013. Volcanological interpretation of historical eruptions of Mt. Baekdusan volcano. J. Korean Earth Sci. Soc. 34, 456–469.

Zou, H.B., Fan, Q.C., Zhang, H.F., Schmitt, A.K., 2014. U-series zircon age constraints on the plumbing system and magma residence times of the Changbai volcano, China/North Korea border. Lithos 200-201, 169–180.